



Published in final edited form as:

Prostate. 2009 September 1; 69(12): 1312–1324. doi:10.1002/pros.20976.

Expression level and DNA methylation status of Glutathione-S-transferase genes in normal murine prostate and TRAMP tumors

Cory K. Mavis, Shannon R. Morey Kinney, Barbara A. Foster, and Adam R. Karpf

Department of Pharmacology and Therapeutics, Roswell Park Cancer Institute, Elm and Carlton Streets, Buffalo, NY 14263

Abstract

BACKGROUND—Glutathione-S-transferase (Gst) genes are down-regulated in human prostate cancer, and GSTP1 silencing is mediated by promoter DNA hypermethylation in this malignancy. We examined Gst gene expression and Gst promoter DNA methylation in normal murine prostates and *Transgenic Adenocarcinoma of Mouse Prostate* (TRAMP) tumors.

METHODS—Primary and metastatic tumors were obtained from TRAMP mice, and normal prostates were obtained from strain-matched WT mice (n=15/group). Quantitative real-time RT-PCR was used to measure *GstA4*, *GstK1*, *GstM1*, *GstO1*, and *GstP1* mRNA expression, and Western blotting and immunohistochemical staining was used to measure GstM1 and GstP1 protein expression. MassARRAY Quantitative Methylation Analysis was used to measure DNA methylation of the 5' CpG islands of *GstA4*, *GstK1*, *GstM1*, *GstO1*, and *GstP1*. TRAMP-C2 cells were treated with the epigenetic remodeling drugs decitabine and trichostatin A (TSA) alone and in combination, and *Gst* gene expression was measured.

RESULTS—Of the genes analyzed, GstM1 and GstP1 were expressed at highest levels in normal prostate. All five Gst genes showed greatly reduced expression in primary tumors compared to normal prostate, but not in tumor metastases. Gst promoter methylation was unchanged in TRAMP tumors compared to normal prostate. Combined decitabine + TSA treatment significantly enhanced the expression of 4/5 Gst genes in TRAMP-C2 cells.

CONCLUSIONS—Gst genes are extensively downregulated in primary but not metastatic TRAMP tumors. Promoter DNA hypermethylation does not appear to drive Gst gene repression in TRAMP primary tumors; however, pharmacological studies using TRAMP cells suggest the involvement of epigenetic mechanisms in Gst gene repression.

Keywords

DNA methylation; TRAMP; Glutathione-S-transferase; prostate cancer

INTRODUCTION

Glutathione S-transferase (Gst) genes are phase II detoxification enzymes that detoxify xenobiotics, environmental carcinogens, and reactive oxygen species (1,2). Gst proteins catalyze the addition of reduced glutathione to substrates to form thioethers (1,3), resulting in the formation of less toxic and reactive products that are targeted for excretion (4). Mammalian

Correspondence: Dr. Adam R. Karpf, Department of Pharmacology and Therapeutics, Roswell Park Cancer Institute, Elm and Carlton Streets, Buffalo, NY 14263, Phone: 716-845-8305, Fax: 716-845-8857; adam.karpf@roswellpark.org.

Disclosure Statement:

The authors declare no competing financial interests.

Gst enzymes are subdivided into three main groups, including a diverse family of cytosolic Gst genes including (Alpha (A) Mu (M), Pi (P), Sigma (S), Theta (T), Zeta (Z), and Omega (O), the mitochondrial GST gene Kappa (K), and microsomal Gst genes, designated MAPEG (4). Increased Gst activity is a response associated with exposure to toxic and foreign compounds and may reduce the mutagenic burden imposed by exposure to these agents (1,5). In support of this idea, GstP1/P2 knockout mice show an increased incidence of 7,12 dimethylbenz[a]anthracene (DMBA)-induced skin tumors (2). Murine tissues that are exposed to increased levels of carcinogens and xenobiotics, including liver and kidney, show higher levels of Gst expression (1). Increased levels of toxic metabolites induce Gst gene expression through the Keap1/Nrf2 pathway, which activates GST gene expression via antioxidant response element (ARE) enhancers found in Gst promoter regions (4). Consistent with this model, Nrf2 null mice display decreased basal expression of multiple Gst genes (6).

In murine chemically-induced carcinogenesis models and human cancer, Gst genes are frequently over-expressed (4,7). However, in contrast to most tumor types, GST genes are frequently down-regulated in human prostate cancer (7,8). Of particular note, GSTP1 is transcriptionally silenced by DNA hypermethylation in human prostate cancer at high frequency and consequently is being developed as a diagnostic marker for prostate cancer (9-19). GSTP1 hypermethylation is an early event during prostate cancer formation, occurring in atrophic hyperplasia and prostatic intraepithelial neoplasia. Functional loss of GSTP1 has been proposed to promote the development of genomic instability and prostate cancer (20). Recently, DNA methylation silencing of Mu-class Gst genes was reported in Barrett's adenocarcinoma, further supporting a role for DNA hypermethylation in Gst gene deregulation in human cancer (21).

DNA methylation is an epigenetic mark that regulates gene expression and plays a critical role in embryonic development, cellular differentiation, and carcinogenesis (22). Moreover, changes in DNA methylation play a key role in cancer (23). In addition to DNA methylation, histone modifications, including lysine acetylation and methylation, are epigenetic regulatory marks that are frequently altered in cancer (24). Epigenetic changes are distinct from genetic mutations in a number of respects, most consequentially in that they are reversible. This reversibility is important both from the standpoint of cancer prevention and treatment, as nutritional and pharmacological agents that prevent or reverse epigenetic gene silencing may have utility in cancer intervention strategies (25,26). In addition, the fact that epigenetic signals are reversible may serve as a mechanism whereby tumor cells can differentially regulate gene expression at distinct stages of tumorigenesis (27).

We and others have recently established *Transgenic Adenocarcinoma of Mouse Prostate* (TRAMP) as a useful *in vivo* model to interrogate the role of epigenetic alterations in prostate cancer (28-32). TRAMP utilizes expression of SV40 early genes driven by the androgen-dependent rat probasin promoter to drive prostate tumorigenesis in the mouse (33). TRAMP displays pathological stages of prostate cancer progression in an age-dependent fashion, and progresses to metastatic tumor growth similar to the human disease (34). In addition, castration of TRAMP animals results in progression to a castration-resistant disease phenotype, as is observed in humans (35). We have previously demonstrated that TRAMP mice display stage-specific alterations in DNA methyltransferase (Dnmt) protein expression, locus- and phenotype-specific DNA hypermethylation, and global DNA hypomethylation, similar to the epigenetic defects observed in human prostate cancer (28,30,31). In addition, Day and colleagues have shown that pharmacological inhibition of DNA methylation prevents prostate cancer formation, delays castration-resistant disease, and extends survival in TRAMP mice (29,32). These studies have validated TRAMP as a useful model for deciphering the contribution of aberrant DNA methylation to prostate cancer.

The goals of the current study were two-fold. First, we sought to determine Gst gene expression levels during tumor progression in TRAMP, to determine whether these genes are downregulated, as has been observed in the human disease. Second, we investigated whether promoter DNA hypermethylation is associated with the silencing of GstP1 and/or other Gst genes in TRAMP. We also utilized TRAMP cells grown *in vitro* to investigate the possibility that Gst genes are epigenetically regulated in this model. Our data indicate that Gst genes are extensively downregulated in primary tumors in the TRAMP model but that this phenotype does not correlate with DNA hypermethylation at proximal promoter regions. However, epigenetic modulatory drugs used in combination led to the activation of specific Gst genes in TRAMP cells, suggesting that additional epigenetic mechanisms beyond DNA methylation likely play a role in Gst gene repression in TRAMP.

MATERIALS AND METHODS

Animals and Tissue Samples

TRAMP 50:50 C57BL/6 × FVB and strain-matched wild-type (WT) animals and tissues have been described previously (31). Samples used in the current study are listed in Table 1. DNA was extracted from 40 mg tissue samples using the Puregene genomic DNA extraction kit (Gentra Systems, Minneapolis, MN). RNA was extracted from 20 mg tissue samples using Trizol (Invitrogen, Carlsbad, CA). Cytosolic protein was extracted from 40 mg tissue samples using the NE-PER Kit (Pierce, Rockford, IL).

Quantitative Real-Time Reverse Transcriptase PCR (qRT-PCR)

qRT-PCR was performed using the 7300 Real-time PCR system (Applied Biosystems, Foster City, CA) as described previously (31), except that absolute quantification of mRNA copy number relative to 18s rRNA was used. Gene-specific *Gst* primers are listed in Supplemental Table 1. Primers for 18s rRNA were described previously (36).

Western Blotting

Western blotting was performed as described previously (31). 20 µg cytosolic protein extracts were loaded per lane. Membranes were probed with the rabbit anti-GstM1 (1:1000) (Upstate Biotechnology, Lake Placid, NY) or polyclonal rabbit anti-GstP1 (1:1500) (MBL laboratories, Naka-ku Nagoya, Japan), followed by donkey anti-rabbit secondary antibody (Amersham Biosciences, Buckinghamshire, England). Band density was quantified using the Versa Doc 5000 Imager System and Quantity One software (BioRad, Hercules, CA) as described (31).

Immunohistochemistry (IHC)

IHC was performed on 5µm sections from paraffin embedded samples of normal prostates from WT mice and primary TRAMP tumors using standard methods. Briefly, endogenous peroxidase was blocked for 15 min at room temperature, using 3% H₂O₂ in methanol. Antigen was retrieved by boiling the slides in Citrate buffer for 20 min. Slides were placed in a humidified chamber with 300µl of 1° polyclonal anti-GstP1 antibody (rabbit 1:2000) or Gstm1 1° polyclonal antibody (1:300), diluted in 1% BSA/1X Tris-P₀₄, and incubated overnight at 4°C. Next, slides were incubated with secondary antibody (donkey α-rabbit (1:100) secondary antibody (Amersham) at room temperature for 2 hrs. Images of representative tissues were obtained using an Olympus IX50 inverted Microscope and Retiga EXi Camera.

MassARRAY Quantitative DNA Methylation Analyses (MAQMA)

MAQMA is a quantitative assay that utilizes matrix-assisted laser desorption/ionization (MALDI) time of flight (TOF) mass spectrometry (MS) and base-specific cleavage to interrogate DNA methylation patterns in sodium-bisulfite converted DNA (37). Primers used

for MAQMA analysis are shown in Supplemental Table 1. Sodium bisulfite conversions were accomplished using the EZ DNA methylation kit (Zymo Research, Orange, CA), and DNA methylation analysis was performed using the MassARRAY system and EpiTYPER software (Sequenom, San Diego, CA). Assay controls included DNA from disease-free mouse whole blood (Clontech, Cat.# 6650-1) as unmethylated control, this same DNA methylated to completion *in vitro* using SssI CpG methylase (New England Biolabs, Beverly, MA) as methylated control, and a 50:50 mix of the unmethylated and methylated control DNAs.

TRAMP-C2 Cells and Drug Treatments

The TRAMP-C2 cell line and its *in vitro* cultivation conditions were described previously (38). Briefly, cells were grown in DMEM media with 10% FBS, 5 ug/ml insulin, 50 units/ml pen-strep, 2 mM L-glutamine, and 10^{-8} M DHT. Cells were treated with 5-aza-2'-deoxycytidine (decitabine) (Sigma, St. Louis, MO) dissolved in PBS and/or Trichostatin A (TSA) (Sigma) solubilized in DMSO. Cells were treated with 1.0 μ M decitabine on day 0 and day 2. On day 4, cells were treated with 600 nM TSA or DMSO control. Cells were harvested on day 5. For TSA-only treatments, cells were treated with 600 nM TSA and harvested one-day (24 hours) post treatment. RNAs were extracted and qRT-PCR analyses for *Gst* gene expression were performed as described above.

RESULTS

Gst mRNA Expression in Normal Mouse Prostate and TRAMP tumors

We initially sought to determine the expression patterns of various *Gst* genes at the mRNA level in normal murine prostate and TRAMP tumors. Of note, a recent study reported that *Gst*-M genes are downregulated in TRAMP (39), but the expression levels of other *Gst* family members in TRAMP are unknown, as are the level of expression of different *Gst* genes in normal murine prostate. To address these questions, we developed quantitative real time RT-PCR (qRT-PCR) assays to measure the expression of five *Gst* genes: *GstA4*, *GstK1*, *GstM1*, *GstO1*, and *GstP1* (Supplemental Table 1). We chose to focus on these five *Gst* genes because GSTP1 silencing is well established in human prostate cancer (12), and a recent microarray study indicated potentially reduced expression of these particular *Gst* genes in T-antigen induced murine tumors ((40) and K.K. Deeb, personal communication). The tissues under study included 15 primary and 15 metastatic tumors from TRAMP animals as well as 15 normal prostates from strain-matched WT animals (Table 1). For the metastatic tumors, we utilized five samples each from kidney, liver, and lymph node metastases (Table 1). For all parameters measured in this study, we obtained virtually identical results for the three different metastatic sites (data not shown), thus these data are combined together into one group in the graphs presented below.

qRT-PCR analysis revealed the relative expression of the five *Gst* genes in normal prostate as *GstM1*>>*GstP1*>*GstO1*>*GstK1*>*GstA4* (Fig 1A). This finding suggests a more prominent role for *GstM1* (and to a lesser extent *GstP1*) in the function of the normal murine prostate as compared to the other *Gst* genes. We next examined *Gst* gene expression in TRAMP primary and metastatic tumors. Strikingly, we observed a similar pattern of expression of each *Gst* gene, with significantly reduced expression in primary tumors, and increased expression (relative to primary tumors and/or normal prostates) in metastatic tumors (Fig. 1B-F). This general pattern held true despite the differences in the basal level of expression of each gene in the normal prostate (Fig. 1A). The uniformly reduced expression of *Gst* genes in TRAMP primary tumors is clearly not an artifact of overall gene expression levels in TRAMP, as our previous studies have demonstrated both increased and decreased expression of genes in TRAMP tumors relative to strain-matched normal prostate in this sample set (30,31).

GstM1 and GstP1 Protein Expression in Normal Mouse Prostate and TRAMP tumors

Based on the data presented above, we performed Western blot analysis to measure the expression of Gst proteins in normal prostate and TRAMP tumors. We focused our attention on GstM1 and GstP1, as antibodies from these proteins were commercially available and because these two genes displayed the highest level of mRNA expression in normal murine prostate. Additionally, GstP1 was of particular interest because it is silenced by DNA hypermethylation in human prostate cancer (12). At the mRNA level, both GstM1 and GstP1 are significantly down-regulated in primary TRAMP tumors but not in metastases (Fig. 1). Fig. 2A-B show results from Western blot analyses of GstM1 and GstP1 protein expression, respectively. As shown, GstM1 and GstP1 are expressed at high levels in normal prostate, and their expression is reduced in primary tumors (Fig. 2A-B). For GstM1, the downregulation was relatively uniform and many tumors showed no observable expression, while for GstP1 downregulation was more variable and approximately one-third of the tumors showed similar levels of expression as normal prostate (Fig. 2). In metastases, GstM1 remains expressed at a lower level than normal prostate, but not as low as seen in primary tumors (Fig. 2A). In contrast, GstP1 does not show reduced protein expression in metastases, and expression is enhanced in some lesions (Fig. 2B).

To confirm our Western blot results, we performed immunohistochemical (IHC) staining of GstM1 and GstP1 in five primary TRAMP tumors along with five strain-matched normal prostates from WT mice. Representative results are shown in Supplemental Fig. 1. Negative control IgG staining of normal ventral prostate showed nuclear hematoxylin staining, but no non-specific staining (Supplemental Fig. 1A-B). In normal ventral prostate both GstM1 and GstP1 were expressed at high level in epithelial cells, with little staining in the stroma (Supplemental Fig. 1A-B). In contrast, TRAMP ventral prostate tumors showed very little staining of either protein (Supplemental Fig. 1A-B). Lateral, dorsal, and anterior prostatic lobes of TRAMP tumors were also examined and these gave similar results (data not shown). We also performed staining on a small set of metastatic tumors and observed variable GstM1 and GstP1 expression, similar to that observed for TRAMP metastases at the mRNA level and by Western blotting (data not shown). Taken together the data indicate that, similar to their mRNAs, GstM1 and GstP1 protein expression is downregulated in primary TRAMP tumors but not in tumor metastases.

DNA Methylation Status of Gst Genes in Normal Mouse Prostate and TRAMP tumors

The data presented above demonstrate that Gst gene expression is highly reduced in TRAMP primary tumors relative to normal murine prostate. GstP1 silencing is the most commonly observed hypermethylation event in human prostate cancer (41). We thus sought to determine whether DNA hypermethylation plays a role in down-regulation of GstP1 and/or other murine Gst genes in TRAMP. Initially, we analyzed the 5' regions of each Gst gene under study, as genes targeted by DNA hypermethylation in cancer contain 5' CpG islands (42). Notably, each Gst gene examined contained a 5' CpG island flanking or upstream of the predicted transcriptional start site (Fig. 3). Based on this finding, we next examined the methylation status of each gene. Given the large number of samples involved in this study (i.e. 45 biological samples \times 5 genes = 225 samples for analysis), we sought a high-throughput and quantitative method for measurement of DNA methylation. For this task, we utilized MassARRAY Quantitative DNA Methylation Analyses (MAQMA) (37). MAQMA allows for quantitative measurement of DNA methylation at CpG sites contained within PCR amplicons from sodium bisulfite converted DNA. MAQMA data can be represented both as the methylation level of individual CpG sites and as the average methylation level over an entire sequenced region.

In normal murine prostate, all five Gst genes displayed a low to moderate level of DNA methylation overall, ranging from 20-40% methylation over the sequenced region (Fig 4A).

For each gene, there was some variability in the methylation level of individual CpG sites within the sequenced region (Fig. 5). Based on the distinct levels of expression of the different Gst genes in normal prostate (Fig. 1A), we examined whether there is an association between Gst gene expression and Gst gene methylation levels in normal prostate. Interestingly, we observed an inverse association between expression and methylation, although GstA4 (which shows the lowest expression in normal prostate) is an outlier (Fig. 4B). When GstA4 is removed from the data set, the correlation coefficient for the inverse association between Gst expression and methylation approaches 1.0 (Fig. 4C). These data suggest that DNA methylation could play a role in regulating Gst gene expression in normal murine prostate tissue although other factors are likely involved.

We also examined Gst promoter methylation in TRAMP tumors. Contrary to our expectation, the overall methylation level of each Gst gene was unchanged in primary tumors and metastases compared to normal prostate (Fig. 6). Despite a lack of overall methylation changes in the 5' CpG islands, hypermethylation of specific critical CpG sites could potentially account for reduced Gst gene expression in primary TRAMP tumors. To test this, we examined the methylation status of individual CpG sites within each promoter region (Fig. 5). For GstA4, two specific CpG sites (site 12 and site 16) showed increased methylation in primary tumors and metastases compared to normal prostate (Fig. 5A). However, as *GstA4* showed reduced expression in primary tumors but increased expression in metastatic tumors relative to normal prostate (Fig. 1B), it is unlikely that the methylation of these sites mediate repression. Importantly, for the other four Gst genes studied, none of the individual CpG sites showed significant methylation differences in TRAMP primary tumors relative to normal prostate from WT mice (Fig. 5B-E).

Pharmacological Inhibition of Epigenetic Enzymes induces Gst gene expression in TRAMP-C2 Cells

While the above data suggested that DNA hypermethylation may not be responsible for the repression of Gst genes in primary TRAMP tumors, we can not exclude the possibility that other epigenetic mechanisms e.g. histone deacetylation could contribute to Gst gene silencing in TRAMP and/or that DNA hypermethylation at cryptic enhancer regions could play a role. Thus, to more comprehensively test potential epigenetic repression of Gst gene in TRAMP, we utilized a pharmacological approach on TRAMP-C2 cells grown *in vitro*. The TRAMP-C2 cell line was established from a primary TRAMP tumor obtained from a 32 week old mouse (38). MAQMA analysis of Gst gene methylation in TRAMP-C2 cells revealed that Gst genes are heterogeneously methylated, similar to that observed in normal prostate and TRAMP tumor samples (data not shown). We treated TRAMP-C2 cells with decitabine, a classical DNA methyltransferase inhibitor (43), and/or TSA, a potent histone deacetylase inhibitor (44) to test the involvement of the respective epigenetic enzymes in Gst gene expression. As shown in Fig. 7, either decitabine or TSA treatment alone did not significantly induce the expression of any of five Gst genes under study, other than a small level of induction of GstA4 with TSA, and a small level of induction of GstO1 with decitabine, respectively. In contrast, combined decitabine + TSA treatment led to significant activation of each Gst gene with the exception of GstM1 (Fig. 7). These data suggest that multiple levels of epigenetic repression are operative on Gst family genes in TRAMP.

DISCUSSION

Here we report the expression and methylation status of Gst genes in a normal murine prostate and murine prostate tumors arising in the TRAMP model. The Gst genes we studied represent 5 key Gst gene classes, including cytosolic (GstA4, GstM1, GstO1, GstP1) and mitochondrial (GstK1) class Gst genes. Of these genes, GstM1 is expressed at the highest levels in normal

murine prostate, followed by GstP1. Using quantitative methods to measure gene expression and promoter DNA methylation, we find that, with the exception of GstA4, there is a strong inverse correlation between Gst gene expression and DNA methylation levels in the normal murine prostate. Most notably, we find that the expression of all five Gst genes studied is dramatically reduced at the mRNA level in primary TRAMP tumors relative to normal prostate. For GstM1 and GstP1, this observation was substantiated at the protein level using both Western blot analyses and IHC.

In contrast to the uniform Gst gene repression observed in primary TRAMP tumors, metastatic TRAMP tumors from three distinct sites (lymph node, liver and kidney) displayed variable levels of Gst gene expression relative to normal prostate, ranging from moderately reduced expression (GstK1) to dramatically increased expression (GstA4). Notably, each Gst gene was expressed at significantly higher levels in tumor metastases relative to primary tumors. We also find that promoter DNA methylation levels of each Gst gene are moderate (~20-40% methylation) in normal prostate and this value was unchanged in TRAMP tumors (either primary or metastatic). This suggests that DNA hypermethylation of Gst genes may not play a primary role in the dramatic repression of these genes observed in primary TRAMP tumors. Importantly, a lack of promoter hypermethylation of Gst genes in primary tumors along with the increased Gst gene expression in metastases may be related. It is possible that DNA hypermethylation, a relatively stable epigenetic lesion, would not be selected for as a chief mechanism for Gst gene repression in primary tumors if enhanced expression of these genes contributes to the transition to metastatic tumor growth.

Our findings of reduced Gst mRNA and protein expression in TRAMP are in agreement with a recent report that the expression of GstM genes and overall Gst enzymatic activity is decreased in TRAMP tumors (39). The fact that Gst genes of numerous classes are repressed in TRAMP tumors suggests the existence of a common underlying mechanism for repression. In this context, a key upstream regulator of Gst genes, Nrf2, is downregulated in TRAMP tumors (39). Prostate epithelial cells derived from Nrf2 null mice were shown to display reduced expression of GstM genes, overall Gst activity, and increased reactive oxygen species relative to control cells (39). Importantly, Nrf2 and GstM expression has been identified to be downregulated in human prostate cancers in microarray studies (39). The mechanism of downregulation of Nrf2 in human prostate cancer and TRAMP is currently unknown, but Frohlich et al reported that the Nrf2 gene is not DNA hypermethylated in TRAMP (39).

Nrf2 regulates Gst gene expression via binding to the antioxidant response element (ARE) found in the promoter or enhancer regions of many Gst genes (4). For the genes investigated in the current study, characterized or non-characterized ARE elements are found in the upstream promoter regions of GstA4, GstM1, and GstP1 (4). For GstA4 and GstP1, the position of the ARE is contained within the region of DNA methylation analysis. Thus although DNA hypermethylation and associated chromatin conformation changes could in theory restrict binding of Nrf2 to hypermethylated Gst promoters, this does not appear to be the mechanism of Gst downregulation in TRAMP tumors. We cannot exclude the possibility that hypermethylation of other upstream regions or cryptic enhancers of Gst genes could contribute to Gst repression in TRAMP. It also remains plausible that other epigenetic changes, e.g. histone modification status, could be altered at Gst ARE sites in TRAMP tumors. Supporting this idea, we find that combined treatment of cultured TRAMP cells with decitabine and TSA induces the expression of multiple Gst genes. Synergistic induction of epigenetically repressed genes by combined treatment with DNMT and HDAC inhibitors is a classical observation, and was noted recently for human GST-M genes (21,45). Chromatin immunoprecipitation analysis of TRAMP tissue samples, while technically challenging, will be required to directly address the involvement of altered histone modifications in Gst gene silencing *in vivo*.

Our finding of an inverse relationship between Gst gene expression and Gst promoter DNA methylation levels in normal murine prostate was unexpected. Whether differential DNA methylation plays a role in regulating gene expression in normal tissues has been actively debated. Interestingly, recent reports have found clear evidence for this phenomenon (46-48). Moreover, a recent study found a significant inverse correlation between human *GSTM5* expression and promoter DNA methylation in normal esophageal mucosa (21). Taken together, these data suggest that DNA methylation may play a role in regulating Gst gene expression in normal tissues. Unlike normal prostate, we did not observe a clear correlation between Gst gene expression in TRAMP tumors and DNA methylation levels (data not shown).

In summary, we demonstrate that reduced Gst gene expression is a common event in primary tumors arising in the TRAMP model, reminiscent of human prostate cancer. Data presented in the current paper as well as other published work suggest a key role for oxidative stress in promoting prostate cancer in TRAMP (39,49). It appears plausible that Nrf2 and Gst gene downregulation plays a major role in the accumulation of oxidative stress in both human and murine prostate cancer. However, in contrast to the human disease, transcriptional silencing of Gst genes does not appear to involve promoter DNA hypermethylation in murine prostate cancer, at least in the TRAMP model, but may involve histone-mediated epigenetic mechanisms, including histone deacetylation. A lack of Gst gene promoter DNA hypermethylation, a relatively stable epigenetic lesion, in primary TRAMP tumors, could be related to the fact that Gst gene expression may need to be reactivated later during tumor progression in order contribute to metastatic tumor growth. Based on our work, further study of the mechanisms involved in Gst gene repression in TRAMP primary tumors, as well as direct assessment of the role of Gst gene downregulation in prostate cancer etiology are warranted.

CONCLUSIONS

Gst genes encode phase II detoxification enzymes that protect the genome from oxidative stress induced DNA damage. Unlike most malignancies, downregulation of Gst genes occurs in human prostate cancer and for at least one of these genes (*GSTP1*), the mechanism of this repression is promoter DNA hypermethylation. We show here that Gst genes from multiple distinct families are repressed in the TRAMP murine prostate cancer model. This repression occurs uniformly in primary TRAMP tumors, but not in tumor metastases taken from three distinct sites. Unlike human prostate cancer, *GstP1* and other Gst genes do not show proximal promoter DNA hypermethylation in either primary or metastatic murine TRAMP tumors. Data from pharmacological experiments using TRAMP cells grown *in vitro* suggest that epigenetic mechanisms in addition to DNA methylation may be involved in Gst gene repression in TRAMP. Taken together, these data suggest that Gst gene downregulation is a common etiological factor in prostate cancer and suggest TRAMP as a useful model to interrogate the role of Gst genes in prostate cancer. While the precise mechanisms leading to Gst downregulation may be distinct in human prostate cancer and TRAMP, in both circumstances it is likely that epigenetic regulatory mechanisms are involved.

Supplementary Material

Refer to Web version on PubMed Central for supplementary material.

Acknowledgments

We are grateful to Kristin Deeb for sharing data prior to publication. We thank Mike Moser, Ellen Karasik, and Bryan Gillard of the RPCI Mouse Tumor Model Resource for assistance with the TRAMP model, Jeff Conroy and Michael Bianchi of the RPCI Microarray and Genomics Resource for assistance with MAMQA analysis, and Petra Link of the Karpf laboratory for assistance with qRT-PCR.

Grant Support: NIH R21CA128062 (ARK), Roswell Park Alliance Foundation (ARK), NIH 5T32CA009072 (SRMK), DOD PC060354 (SRMK), NCI Center Grant CA16056 (Roswell Park Cancer Institute).

Abbreviations

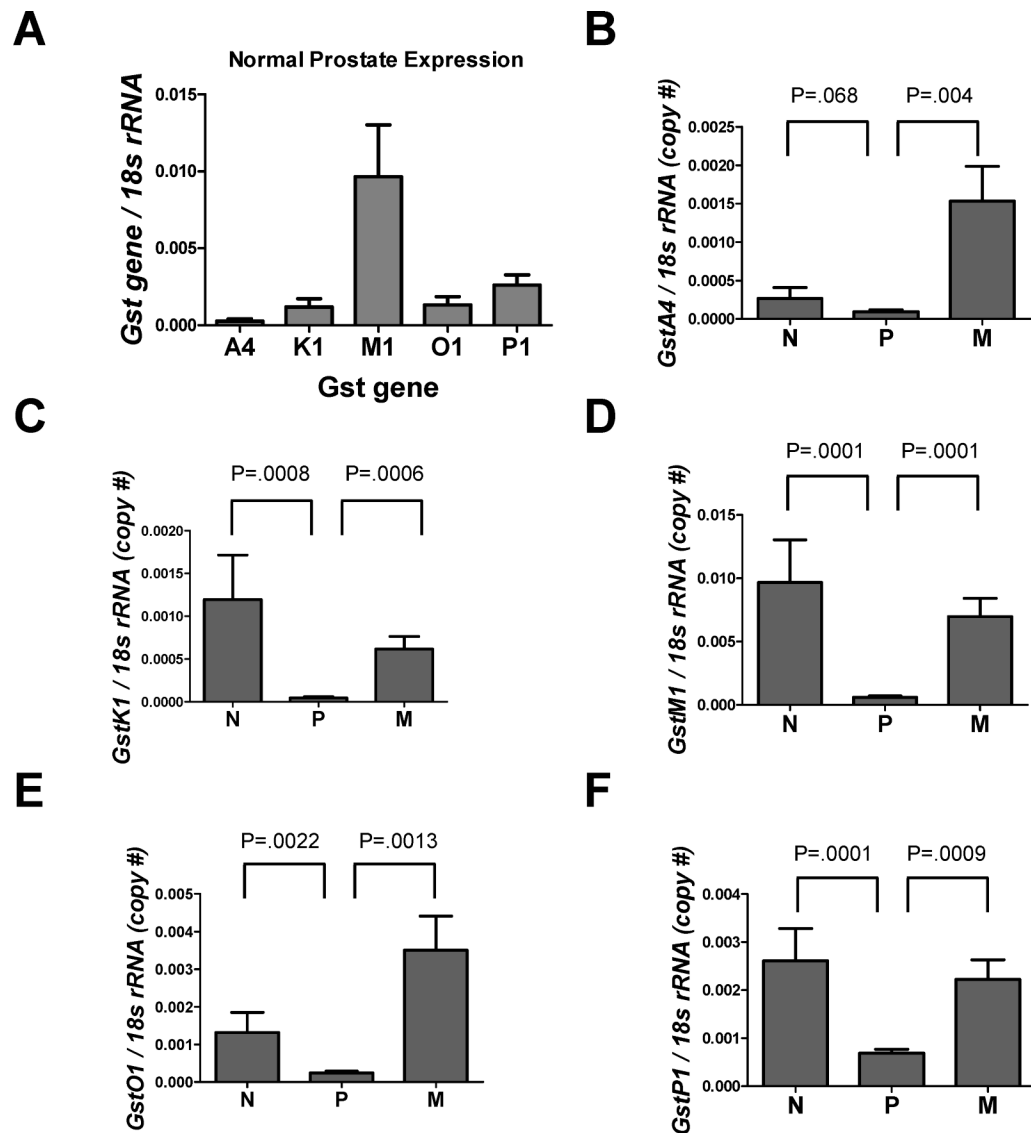
| | |
|-------|---|
| Gst | Murine Glutathione-S-transferase gene |
| TRAMP | transgenic adenocarcinoma of mouse prostate |
| DNMT | cytosine DNA methyltransferase |

REFERENCES

- Hayes JD, Pulford DJ. The glutathione S-transferase supergene family: regulation of GST and the contribution of the isoenzymes to cancer chemoprotection and drug resistance. *Crit Rev Biochem Mol Biol* 1995;30(6):445–600. [PubMed: 8770536]
- Herderson CJ, Smith IR, Rushmore TH, Crane TL, Thorn C, Kocal TE, Ferguson HW. Increased skin tumorigenesis in mice lacking pi class glutathione S-transferases. *Proc Natl Acad Sci* 1998;95:5275–5280. [PubMed: 9560266]
- Rushmore TH, Pickett CB. Glutathione S-transferases, structure, regulation, and therapeutic implications. *J Biol Chem* 1993;268(16):11475–11478. [PubMed: 8505281]
- Hayes JD, Flanagan JU, Jowsey IR. Glutathione transferases. *Annu Rev Pharmacol Toxicol* 2005;45:51–88. [PubMed: 15822171]
- Bostwick DG, Burke HB, Djakiew D, Euling S, Ho SM, Landolph J, Morrison H, Sonawane B, Shifflett T, Waters DJ, Timms B. Human prostate cancer risk factors. *Cancer* 2004;101(10 Suppl):2371–2490. [PubMed: 15495199]
- Hayes JD, Chanas SA, Henderson CJ, McMahon M, Sun C, Moffat GJ, Wolf CR, Yamamoto M. The Nrf2 transcription factor contributes both to the basal expression of glutathione S-transferases in mouse liver and to their induction by the chemopreventive synthetic antioxidants, butylated hydroxyanisole and ethoxyquin. *Biochemical Society transactions* 2000;28(2):33–41. [PubMed: 10816095]
- Bostwick DG, Meiers I, Shanks JH. Glutathione S-transferase: differential expression of alpha, mu, and pi isoenzymes in benign prostate, prostatic intraepithelial neoplasia, and prostatic adenocarcinoma. *Human pathology* 2007;38(9):1394–1401. [PubMed: 17555796]
- Nakayama M, Gonzalgo ML, Yegnasubramanian S, Lin X, De Marzo AM, Nelson WG. GSTP1 CpG island hypermethylation as a molecular biomarker for prostate cancer. *Journal of cellular biochemistry* 2004;91(3):540–552. [PubMed: 14755684]
- Lee WH, Morton RA, Epstein JI, Brooks JD, Campbell PA, Bova GS, Hsieh WS, Isaacs WB, Nelson WG. Cytidine methylation of regulatory sequences near the pi-class glutathione S-transferase gene accompanies human prostatic carcinogenesis. *Proc Natl Acad Sci U S A* 1994;91(24):11733–11737. [PubMed: 7972132]
- Li LC, Carroll PR, Dahiya R. Epigenetic changes in prostate cancer: implication for diagnosis and treatment. *J Natl Cancer Inst* 2005;97(2):103–115. [PubMed: 15657340]
- Papadopoulou E, Davilas E, Sotiriou V, Georgakopoulos E, Georgakopoulou S, Koliopoulos A, Aggelakis F, Dardoufas K, Agnanti NJ, Karydas I, Nasioulas G. Cell-free DNA and RNA in plasma as a new molecular marker for prostate and breast cancer. *Ann N Y Acad Sci* 2006;1075:235–243. [PubMed: 17108217]
- Lin X, Tascilar M, Lee WH, Vles WJ, Lee BH, Veeraswamy R, Asgari K, Freije D, van Rees B, Gage WR, Bova GS, Isaacs WB, Brooks JD, DeWeese TL, De Marzo AM, Nelson WG. GSTP1 CpG island hypermethylation is responsible for the absence of GSTP1 expression in human prostate cancer cells. *The American journal of pathology* 2001;159(5):1815–1826. [PubMed: 11696442]
- Maruyama R, Toyooka S, Toyooka KO, Virmani AK, Zochbauer-Muller S, Farinas AJ, Minna JD, McConnell J, Frenkel EP, Gazdar AF. Aberrant promoter methylation profile of prostate cancers and its relationship to clinicopathological features. *Clin Cancer Res* 2002;8(2):514–519. [PubMed: 11839671]

14. Yamanaka M, Watanabe M, Yamada Y, Takagi A, Murata T, Takahashi H, Suzuki H, Ito H, Tsukino H, Katoh T, Sugimura Y, Shiraishi T. Altered methylation of multiple genes in carcinogenesis of the prostate. *International journal of cancer* 2003;106(3):382–387.
15. Jeronimo C, Henrique R, Hoque MO, Mambo E, Ribeiro FR, Varzim G, Oliveira J, Teixeira MR, Lopes C, Sidransky D. A quantitative promoter methylation profile of prostate cancer. *Clin Cancer Res* 2004;10(24):8472–8478. [PubMed: 15623627]
16. Kang GH, Lee S, Lee HJ, Hwang KS. Aberrant CpG island hypermethylation of multiple genes in prostate cancer and prostatic intraepithelial neoplasia. *The Journal of pathology* 2004;202(2):233–240. [PubMed: 14743506]
17. Singal R, Ferdinand L, Reis IM, Schlesselman JJ. Methylation of multiple genes in prostate cancer and the relationship with clinicopathological features of disease. *Oncology reports* 2004;12(3):631–637. [PubMed: 15289848]
18. Woodson K, Gillespie J, Hanson J, Emmert-Buck M, Phillips JM, Linehan WM, Tangrea JA. Heterogeneous gene methylation patterns among pre-invasive and cancerous lesions of the prostate: a histopathologic study of whole mount prostate specimens. *Prostate* 2004;60(1):25–31. [PubMed: 15129426]
19. Yegnasubramanian S, Kowalski J, Gonzalgo ML, Zahurak M, Piantadosi S, Walsh PC, Bova GS, De Marzo AM, Isaacs WB, Nelson WG. Hypermethylation of CpG islands in primary and metastatic human prostate cancer. *Cancer Res* 2004;64(6):1975–1986. [PubMed: 15026333]
20. De Marzo AM, Platz EA, Sutcliffe S, Xu J, Gronberg H, Drake CG, Nakai Y, Isaacs WB, Nelson WG. Inflammation in prostate carcinogenesis. *Nature reviews* 2007;7(4):256–269.
21. Peng DF, Razvi M, Chen H, Washington K, Roessner A, Schneider-Stock R, El-Rifai W. DNA hypermethylation regulates the expression of members of the Mu-class glutathione S-transferases and glutathione peroxidases in Barrett's adenocarcinoma. *Gut* 2009;58(1):5–15. [PubMed: 18664505]
22. Bird A. DNA methylation patterns and epigenetic memory. *Genes & development* 2002;16(1):6–21. [PubMed: 11782440]
23. Feinberg AP, Tycko B. The history of cancer epigenetics. *Nature reviews* 2004;4(2):143–153.
24. Esteller M. Epigenetics in cancer. *The New England journal of medicine* 2008;358(11):1148–1159. [PubMed: 18337604]
25. Fang M, Chen D, Yang CS. Dietary polyphenols may affect DNA methylation. *The Journal of nutrition* 2007;137(1 Suppl):223S–228S. [PubMed: 17182830]
26. Karpf AR, Jones DA. Reactivating the expression of methylation silenced genes in human cancer. *Oncogene* 2002;21(35):5496–5503. [PubMed: 12154410]
27. Graff JR, Gabrielson E, Fujii H, Baylin SB, Herman JG. Methylation patterns of the E-cadherin 5' CpG island are unstable and reflect the dynamic, heterogeneous loss of E-cadherin expression during metastatic progression. *J Biol Chem* 2000;275(4):2727–2732. [PubMed: 10644736]
28. Camoriano M, Kinney SR, Moser MT, Foster BA, Mohler JL, Trump DL, Karpf AR, Smiraglia DJ. Phenotype-specific CpG island methylation events in a murine model of prostate cancer. *Cancer Res* 2008;68(11):4173–4182. [PubMed: 18519676]
29. McCabe MT, Low JA, Daignault S, Imperiale MJ, Wojno KJ, Day ML. Inhibition of DNA methyltransferase activity prevents tumorigenesis in a mouse model of prostate cancer. *Cancer Res* 2006;66(1):385–392. [PubMed: 16397253]
30. Morey Kinney SR, Smiraglia DJ, James SR, Moser MT, Foster BA, Karpf AR. Stage-specific alterations of DNA methyltransferase expression, DNA hypermethylation, and DNA hypomethylation during prostate cancer progression in the transgenic adenocarcinoma of mouse prostate model. *Mol Cancer Res* 2008;6(8):1365–1374. [PubMed: 18667590]
31. Morey SR, Smiraglia DJ, James SR, Yu J, Moser MT, Foster BA, Karpf AR. DNA methylation pathway alterations in an autochthonous murine model of prostate cancer. *Cancer Res* 2006;66(24):11659–11667. [PubMed: 17178860]
32. Zorn CS, Wojno KJ, McCabe MT, Kuefer R, Gschwend JE, Day ML. 5-aza-2'-deoxycytidine delays androgen-independent disease and improves survival in the transgenic adenocarcinoma of the mouse prostate mouse model of prostate cancer. *Clin Cancer Res* 2007;13(7):2136–2143. [PubMed: 17404097]

33. Greenburg NM, DeMayo F, Finegold MJ, Medina D, Tilley WD, Aspinall JO, Cunha GR, Donjacour AA, Matusik RJ, Rosen JM. Prostate cancer in a transgenic mouse. *Proc Natl Acad Sci* 1995;3439–3443. [PubMed: 7724580]
34. Gingrich JR, Barrios RJ, Foster BA, Greenberg NM. Pathologic progression of autochthonous prostate cancer in the TRAMP model. *Prostate Cancer Prostatic Dis* 1999;2(2):70–75. [PubMed: 12496841]
35. Gingrich JR, Barrios RJ, Kattan MW, Nahm HS, Finegold MJ, Greenberg NM. Androgen-independent prostate cancer progression in the TRAMP model. *Cancer Res* 1997;57(21):4687–4691. [PubMed: 9354422]
36. Schmittgen TDZB. Effect of experimental treatment on housekeeping gene expression: validation by real-time, quantitative RT-PCR. *J Biochem Biophys Methods* 2000;46:69–81. [PubMed: 11086195]
37. Ehrich M, Nelson MR, Stanssens P, Zabeau M, Liloglou T, Xinarianos G, Cantor CR, Field JK, van den Boom D. Quantitative high-throughput analysis of DNA methylation patterns by base-specific cleavage and mass spectrometry. *Proc Natl Acad Sci U S A* 2005;102(44):15785–15790. [PubMed: 16243968]
38. Foster BA, Gingrich JR, Kwon ED, Madias C, Greenberg NM. Characterization of prostatic epithelial cell lines derived from transgenic adenocarcinoma of the mouse prostate (TRAMP) model. *Cancer Res* 1997;57(16):3325–3330. [PubMed: 9269988]
39. Frohlich DA, McCabe MT, Arnold RS, Day ML. The role of Nrf2 in increased reactive oxygen species and DNA damage in prostate tumorigenesis. *Oncogene* 2008;27(31):4353–4362. [PubMed: 18372916]
40. Deeb KK, Michalowska AM, Yoon CY, Krummey SM, Hoenerhoff MJ, Kavanaugh C, Li MC, Demayo FJ, Linnoila I, Deng CX, Lee EY, Medina D, Shih JH, Green JE. Identification of an integrated SV40 T/t-antigen cancer signature in aggressive human breast, prostate, and lung carcinomas with poor prognosis. *Cancer Res* 2007;67(17):8065–8080. [PubMed: 17804718]
41. Meiers I, Shanks JH, Bostwick DG. Glutathione S-transferase pi (GSTP1) hypermethylation in prostate cancer: review 2007. *Pathology* 2007;39(3):299–304. [PubMed: 17558856]
42. Baylin SB, Herman JG, Graff JR, Vertino PM, Issa JP. Alterations in DNA methylation: a fundamental aspect of neoplasia. *Advances in cancer research* 1998;72:141–196. [PubMed: 9338076]
43. Jones PA, Taylor SM. Cellular differentiation, cytidine analogs and DNA methylation. *Cell* 1980;20(1):85–93. [PubMed: 6156004]
44. Yoshida M, Kijima M, Akita M, Beppu T. Potent and specific inhibition of mammalian histone deacetylase both in vivo and in vitro by trichostatin A. *J Biol Chem* 1990;265(28):17174–17179. [PubMed: 2211619]
45. Cameron EE, Bachman KE, Myohanen S, Herman JG, Baylin SB. Synergy of demethylation and histone deacetylase inhibition in the re-expression of genes silenced in cancer. *Nature genetics* 1999;21(1):103–107. [PubMed: 9916800]
46. Song F, Mahmood S, Ghosh S, Liang P, Smiraglia DJ, Nagase H, Held WA. Tissue specific differentially methylated regions (TDMR): Changes in DNA methylation during development. *Genomics* 2009;93(2):130–139. [PubMed: 18952162]
47. Song F, Smith JF, Kimura MT, Morrow AD, Matsuyama T, Nagase H, Held WA. Association of tissue-specific differentially methylated regions (TDMs) with differential gene expression. *Proc Natl Acad Sci U S A* 2005;102(9):3336–3341. [PubMed: 15728362]
48. Suzuki M, Sato S, Arai Y, Shinohara T, Tanaka S, Grealley JM, Hattori N, Shiota K. A new class of tissue-specifically methylated regions involving entire CpG islands in the mouse. *Genes Cells* 2007;12(12):1305–1314. [PubMed: 18076568]
49. Tam NN, Nyska A, Maronpot RR, Kissling G, Lomnitski L, Suttie A, Bakshi S, Bergman M, Grossman S, Ho SM. Differential attenuation of oxidative/nitrosative injuries in early prostatic neoplastic lesions in TRAMP mice by dietary antioxidants. *The Prostate* 2006;66(1):57–69. [PubMed: 16114064]

**Fig. 1.**

Gst mRNA expression in normal prostates from WT mice and TRAMP tumors. qRT-PCR of *Gst* genes was performed as described in *Materials and Methods* using the samples described in Table 1. *Gst* mRNA copy number is plotted relative to 18s rRNA expression. (A) *Gst* expression in normal murine prostate (N = 15). *Gst* family members analyzed are shown on the x-axis. (B) *GstA4* (C) *GstK1* (D) *GstM1* (E) *GstO1* and (F) *GstP1* mRNA expression in normal prostate (N), primary prostate tumor (P), and metastases (M) (N = 15/group). The metastases group includes lymph node, kidney, and liver metastases (5 each). Error bars = Standard deviation (SD). The results of unpaired two-tailed T-test comparisons are shown for the indicated groups. In all cases, differences in *Gst* mRNA expression between Normal Prostate and Metastatic tumors were not significant.

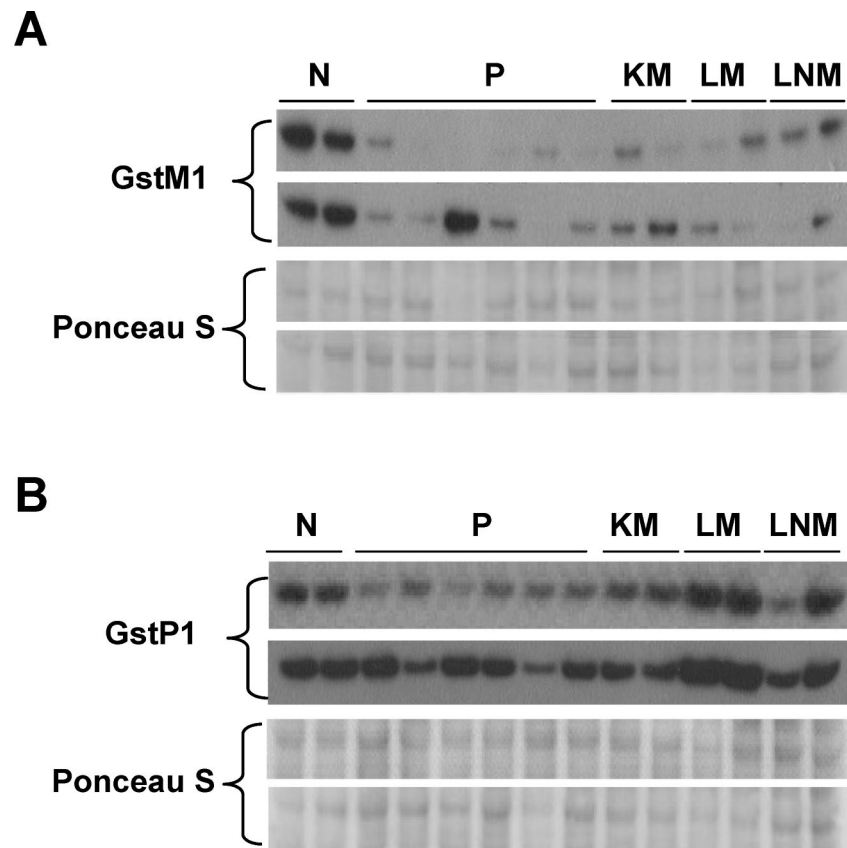


Fig. 2. Western blot analysis of Gstm1 and Gstp1 protein expression in normal prostates from WT mice and TRAMP tumors. Cytosolic Gstm1 and Gstp1 protein levels were measured as described in *Materials and Methods* using the samples described in Table 1; representative Western blots are shown. **(A)** Gstm1 Western blots. **(B)** Gstp1 Western blots. Data labels: Normal prostates (N), primary tumors (P), kidney metastases (KM), liver metastases (LM), and lymph node metastases (LNM). For both panels, Ponceau S total protein staining served as a loading control.

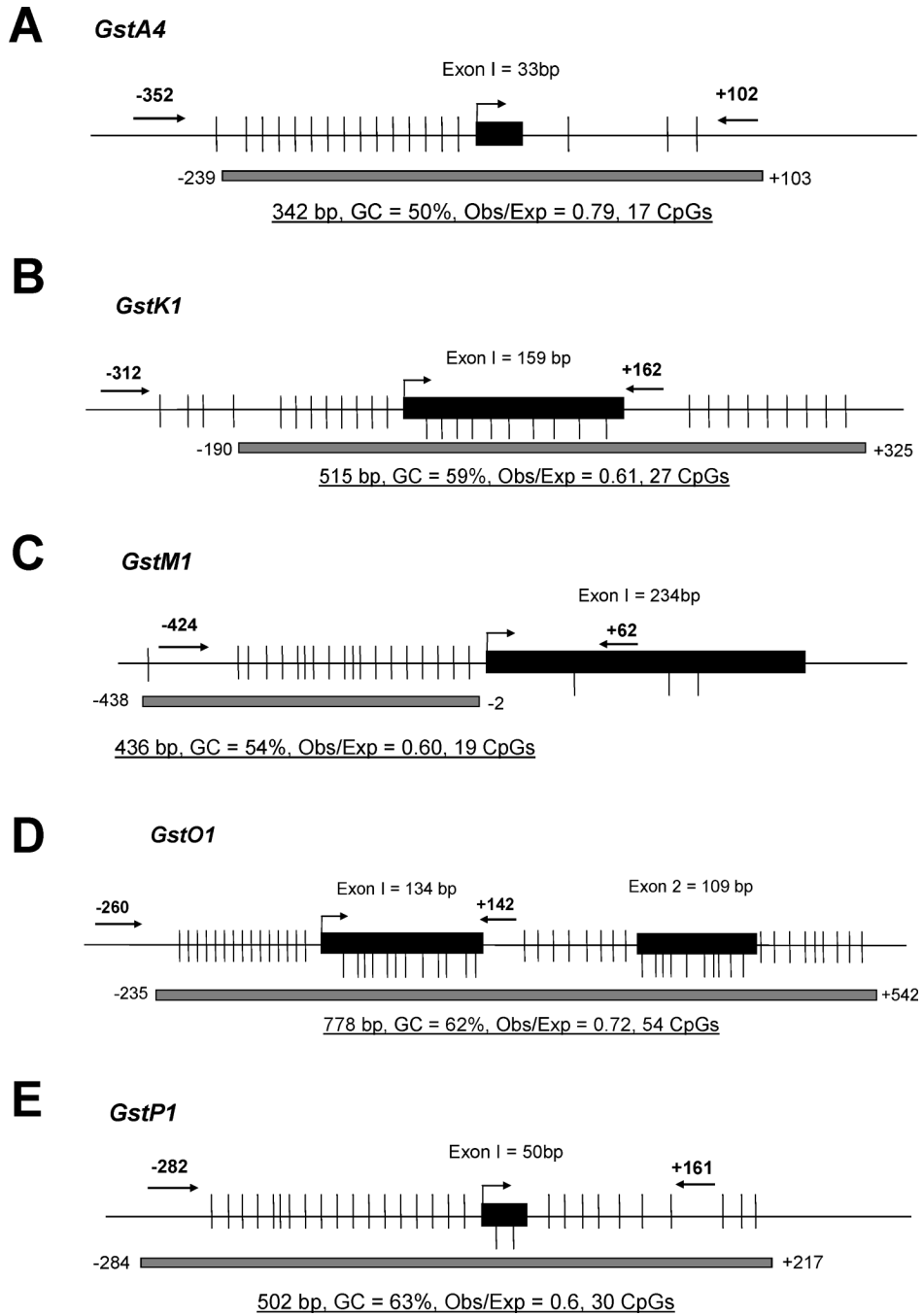


Fig. 3. 5' end of murine *Gst* genes, indicating position of CpG islands and primer sites used for DNA methylation analyses. (A) *Gsta4*, (B) *Gstk1*, (C) *Gstm1*, (D) *Gsto1*, and (E) *Gstp1*. For each diagram, the predicted transcriptional start sites from the UC Santa Cruz Genome Browser are shown with bent right arrows, and exons are shown with black filled bars. Hash marks indicate CpG sites. Gray filled bars show 5' CpG islands; CpG island characteristics as determined using CpG island searcher (<http://www.uscnorris.com/cpgislands2/cpg.aspx>) are shown beneath the gray bars. The approximate position and 5' nucleotide coordinates of primers used for MAQMA methylation analysis are shown by inward facing arrows.

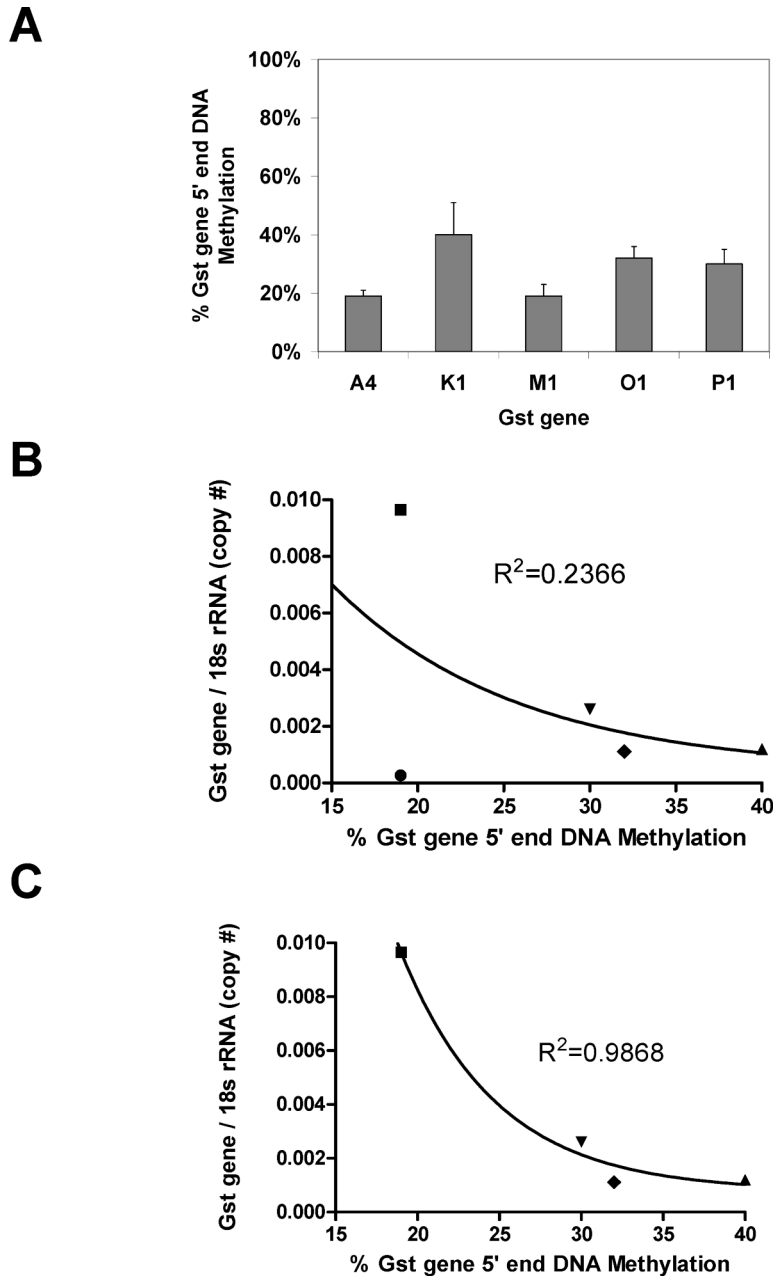


Fig. 4. Gst gene methylation in normal murine prostate and inverse association with *Gst* mRNA expression. (A) DNA methylation of the 5' regions of Gst genes diagrammed in Fig. 4 were determined by MassARRAY Quantitative DNA Methylation Analyses (MAQMA) as described in the *Materials and Methods*. Results plotted are the average methylation value of all CpG sites over the entire sequenced region, and all data are averaged over 5 normal prostate samples. Error bars = SD. (B) Gst methylation values plotted against *Gst* mRNA expression values shown in Fig. 1A. Non-linear regression (one-phase decay) correlation coefficient R^2 value was calculated using GraphPad Prism and is shown. (C) Gst methylation values plotted against *Gst* mRNA expression values shown in Fig. 1A, after removal of GstA4 data. Correlation coefficient R^2 value was calculated as described in panel C. Symbols : square = GstM1; circle = GstA4; inverted triangle = GstP1; diamond = GstO1; triangle = GstK1.

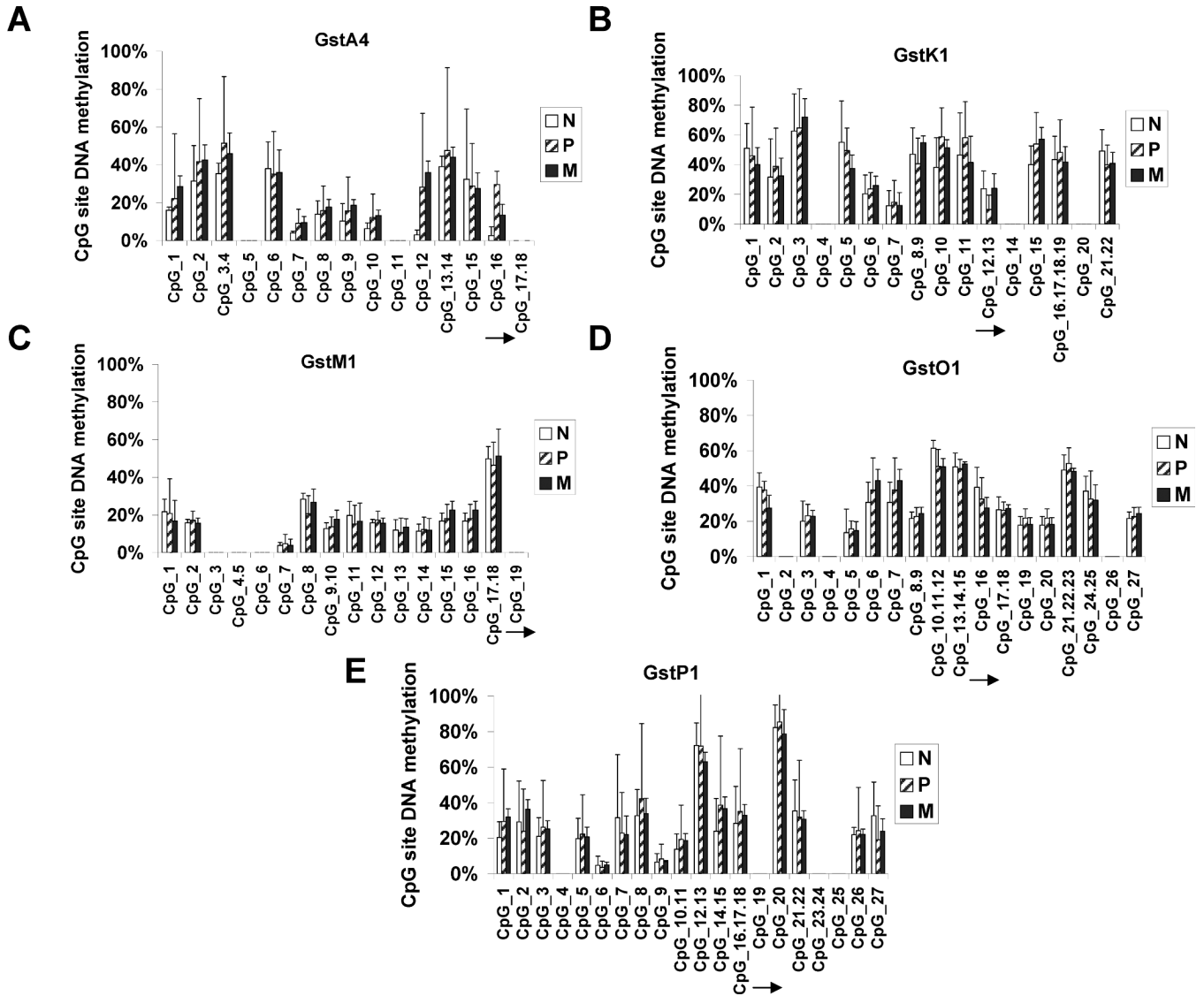


Fig. 5. Individual CpG site DNA methylation of *Gst* genes in normal prostates from WT mice and TRAMP tumors. (A) *GstA4*, (B) *GstK1*, (C) *GstM1*, (D) *GstO1*, and (E) *GstP1*. DNA methylation of the 5' regions of *Gst* genes diagrammed in Fig. 3 were determined by MassARRAY Quantitative DNA Methylation Analyses (MAQMA) as described in the *Materials and Methods*. Results plotted are the average methylation value of each CpG site (or clusters of CpG sites) within each sequenced region, and data are averaged for normal prostate (N) (N=5), primary tumor (P) (N=15), and metastatic tumors (M) (N = 15). Infrequently, CpG sites failed MAQMA analysis; in these instances no data are shown (absence of bars on the graph). Right arrows below X-axes indicate the approximate position of the predicted transcriptional start site for each gene. Error bars = SD.

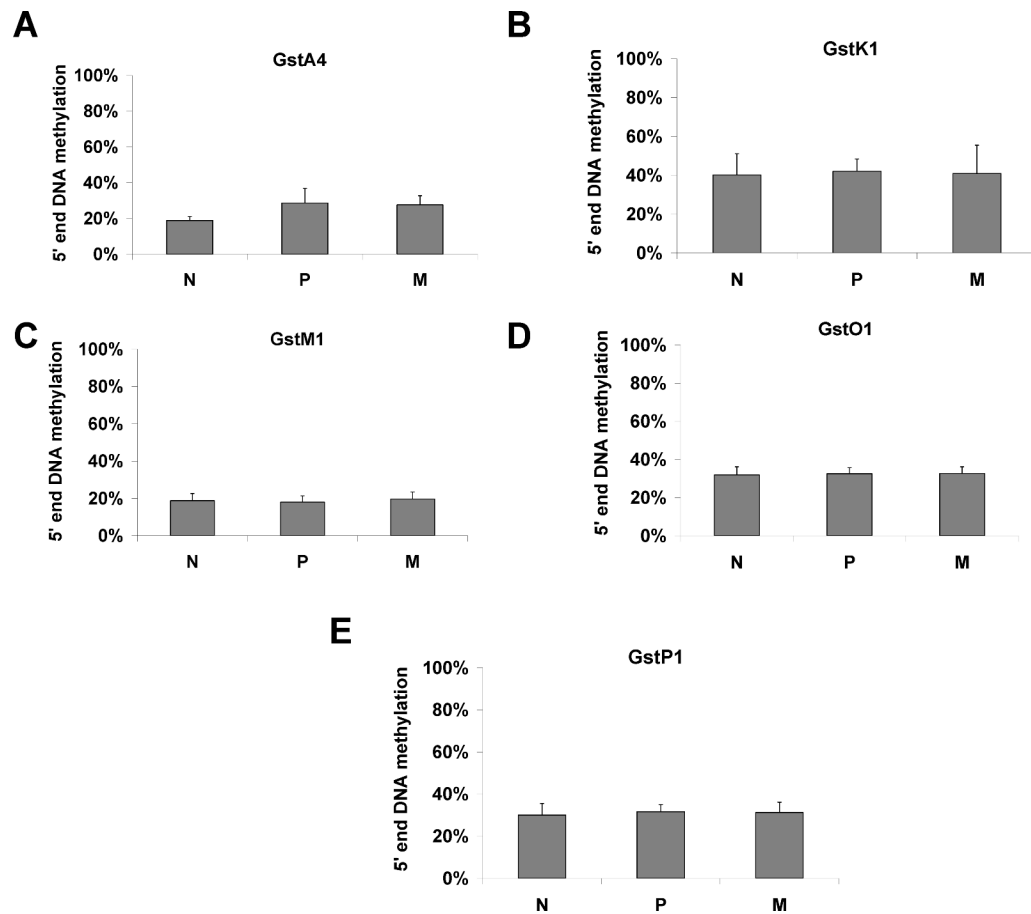


Fig. 6. Averaged Gst gene methylation in normal prostates from WT mice and TRAMP tumors. **(A)** *GstA4*, **(B)** *GstK1*, **(C)** *GstM1*, **(D)** *GstO1*, and **(E)** *GstP1*. DNA methylation of the 5' regions of Gst genes diagrammed in Fig. 3 were determined by MassARRAY Quantitative DNA Methylation Analyses (MAQMA) as described in the *Materials and Methods*. Results plotted are the average methylation value of all CpG sites over the entire sequenced region, and all data are averaged for normal prostates (N) (N=5), primary tumors (P) (N=15), and metastatic tumors (M) (N = 15). The methylation data for the individual sites comprising each region are shown in Fig. 5. Error bars = SD. In all cases, the differences between groups were not significant (data not shown).

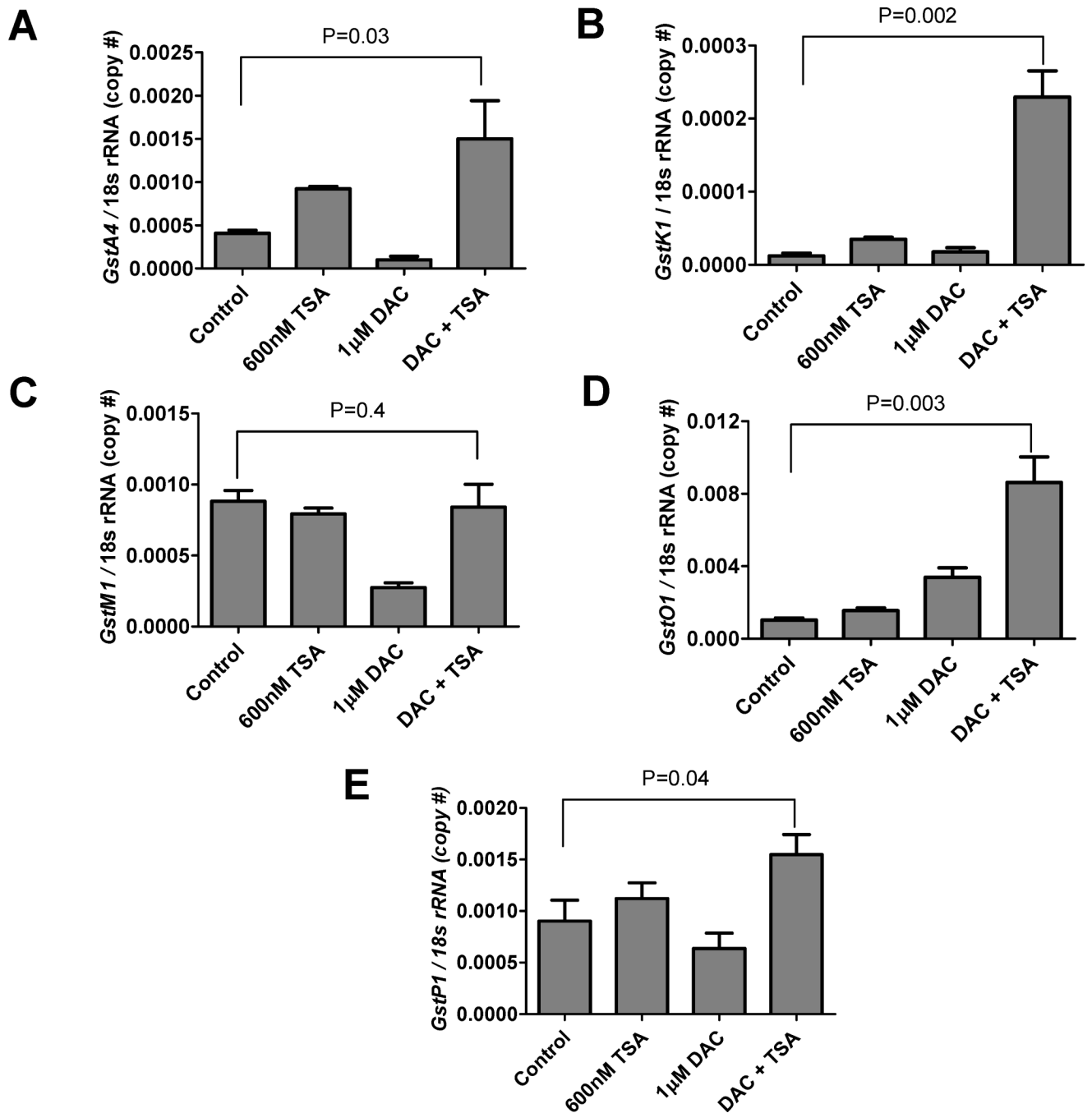


Fig. 7. Effect of decitabine and TSA treatment on Gst gene expression in TRAMP-C2 cells. TRAMP-C2 cells were treated with 1.0 µM decitabine (DAC) and/or 600 nM trichostatin A (TSA) as described in the *Materials and Methods*, and cells were harvest at five days post-DAC treatment and/or one day post TSA treatment. The vehicle control consisted of treatment of TRAMP-C2 cells with PBS and DMSO for five days and one day, respectively. Gst mRNA expression was measured by qRT-PCR as described in the *Materials and Methods*. **(A)** *GstA4*, **(B)** *GstK1*, **(C)** *GstM1*, **(D)** *GstO1*, and **(E)** *GstP1*. Error bars = SD. Students T-test (unpaired, one-tailed) was performed to test for significant differences in Gst gene expression between control cells and cells treated with DAC and TSA. Results (P-values) are shown on the figure.

Table 1

Samples used.

| Tissue Type | Mouse Strain | # of Samples | Age (weeks \pm SD) | Urogenital Tract Weight (mgs \pm SD) | Prostate Weight (mgs \pm SD) |
|-----------------------|---------------------------------|--------------|----------------------|--|--------------------------------|
| Normal | 50:50 C57Bl/6:FVB Wildtype (WT) | 15 | 22.9 \pm 8.0 | 0.57 \pm 0.2 | 0.02 \pm 0.00 |
| Primary Tumor | " " TRAMP | 15 | 25.9 \pm 4.5 | 6.21 \pm 2.5 | 5.67 \pm 3.8 |
| Kidney Metastasis | " " TRAMP | 5 | 26.8 \pm 6.9 | 6.51 \pm 10.7 | 9.12 \pm 13.8 |
| Liver Metastasis | " " TRAMP | 5 | 26.4 \pm 8.3 | 3.97 \pm 4.2 | 2.00 \pm 4.2 |
| Lymph Node Metastasis | " " TRAMP | 5 | 31.8 \pm 6.5 | 7.95 \pm 6.2 | 7.93 \pm 7.0 |